Available online at www.sciencedirect.com
ScienceDirect
Journal of Sound and Vibration 311 (2008) 737–755
JOURNAL OF SOUND AND VIBRATION
www.elsevier.com/locate/jsvi

Modal analysis of mdof system by using free vibration response data only

Bor-Tsuen Wang*, Deng-Kai Cheng

Department of Mechanical Engineering, National Pingtung University of Science and Technology, Pingtung 91201, Taiwan

Received 2 November 2006; received in revised form 14 July 2007; accepted 24 September 2007
Available online 29 October 2007

Abstract

Conventional modal testing requires the actuator and sensor to perform FRF measurement so as to determine the structural modal parameters. This paper presents a new idea of experimental modal analysis by only using the structural free vibration response due to initial conditions. If the structural displacement can be measured, the displacement response matrices that are the discrete-time-domain data for all measured dofs can be formulated. The velocity and acceleration response matrices can then be calculated by finite difference methods. With the input of these response matrices to the developed algorithm, the system natural frequencies and their corresponding mode shapes can be determined simultaneously. Numerical examples for a 3-dof and 10-dof systems are presented, to show, respectively, the feasibility and effectiveness of the developed method. Results show the proposed method is very promising. Only the structural displacement response in free vibration condition need to be measured and as the input to the modal parameter extraction algorithm such that all of the structural modal frequencies and mode shapes of the system can be determined successfully. The presented idea can also be extended and applied to the general structure with non-proportional damping case. The proposed methodology can therefore enhance the structural modal analysis technique.

1. Introduction

Experimental modal analysis (EMA) or modal testing is an important engineering technique to experimentally determine the structural modal parameters. And EMA can be combined with computer-aided engineering (CAE) that provides theoretical simulation to verify the structural theoretical model, and so forth the virtual testing [1] can be implemented to assist product design and development. However, conventional EMA has some limitations, such as the test structure in static condition, the requirement of controllable input excitation source and the involvement of sophisticated curve-fitting numerical process. Operational modal analysis (OMA), output-only modal analysis (OOMA), or natural input modal analysis (NIMA) is greatly interested to improve the above-mentioned limitations. This work thus intends to develop the modal analysis algorithm by using free vibration response only to overcome the conventional EMA limitation.

*Corresponding author. Tel.: +886 8 770 3202x7017; fax: +886 8 7740 0142.
E-mail address: wangbt@mail.npust.edu.tw (B.-T. Wang).

0022-460X/$ - see front matter
doi:10.1016/j.jsv.2007.09.030

Nomenclature

$\mathbf{C}$	damping matrix
$\mathbf{D}_1$	differential transformation matrix from displacement to velocity
$\mathbf{D}_2$	differential transformation matrix from velocity to acceleration
f_s	sampling frequency (Hz)
f_r	rth natural frequency (Hz)
$\hat{f}_r$	predicted rth natural frequency (Hz)
$\mathbf{f}$	force vector
k	started number of time-domain response data point for MAFVRO algorithm
$\mathbf{K}$	stiffness matrix
m_r	rth modal mass
MAC	modal assurance criterion
$\mathbf{M}$	mass matrix
n	number of dofs
N_k	number of data points for response matrix
$\mathbf{q}(t)$	modal coordinate vector
$q_r(t)$	rth modal coordinate
q_{r0}	initial displacement for the rth modal coordinate
$\dot{q}_{r0}$	initial velocity for the rth modal coordinate
$\mathbf{q}_0$	initial displacement vector for modal coordinate
$\dot{\mathbf{q}}_0$	initial velocity vector for modal coordinate
RAN	normally distributed random number between -1 and 1
SNR	signal-to-noise ratio
$\mathbf{v}_0$	initial velocity vector
$x_r(t_k) = x_{r,k}$	displacement of the rth dof at time t_k
$\mathbf{x}$	displacement vector
$\dot{\mathbf{x}}$	velocity vector
$\ddot{\mathbf{x}}$	acceleration vector
$\mathbf{x}_0$	initial displacement vector
$\mathbf{X}_r$	rth mode shape vector
$\mathbf{X}$	displacement response matrix
$\dot{\mathbf{X}}$	velocity response matrix
$\ddot{\mathbf{X}}$	acceleration response matrix
α, β	some constant for proportional damping
Δt	discrete time interval
ε_r	percentage of prediction error for the rth natural frequency
$\boldsymbol{\phi}_r$	rth mass-matrix normalized mode shape vector
$\hat{\boldsymbol{\phi}}_r$	predicted rth mass-matrix normalized mode shape vector
$\boldsymbol{\Phi}$	modal matrix
ω_{dr}	rth damped natural frequency (rad/s)
ω_r	rth natural frequency (rad/s)
ξ_r	rth damping ratio

Kim et al. [2] revised Ibrahim time-domain (ITD) method [3] and developed time-domain decomposition (TDD) from sdof transient response. They used output-only response signal through the band pass filter and performed singular value decomposition (SVD) to determine structural modal model suitable for arbitrary types of force excitation. Brinker et al. [4] adopted the frequency-domain decomposition (FDD) method by processing the output power spectral matrix and employing SVD to extract structural modal parameters with the assumption of white-noise excitation. Shen et al. [5] utilized the cross power spectral density function and correlation function to replace frequency response function (FRF) and impulse response function (IRF), respectively, from the output-only response data to obtain structural modal parameters. And, the structure is also assumed subject to white-noise excitation.

In practice, the white noise excitation assumption may not be sufficient to be applied. Mohanty and Rixen [6] considered both harmonic and white noise excitation as coexisting and developed single station time domain (SSTD) method [7] to perform modal analysis of structures in operating conditions. Mohanty and Rixen [8] also modified and applied least-square complex exponential (LSCE) method to determine modal parameters of beam structure in harmonic response.

Stochastic subspace identification (SSI) method is another frequently adopted approach to perform OMA. Yu and Ren [9] developed their SSI method based on empirical mode decomposition (EMD) to measure only time-domain response of the structure subject to random excitation. Without the frequency-domain data they had successfully applied to civil structures for structural model identification.

This work is inspired from Zhou and Chelidze [10] who assumed to measure the free vibration response data and adopted smooth orthogonal decomposition (SOD) method to extract normal modes of discrete system.

Feeny and Kappagantu [11] can be the first to discuss the modal analysis for structure in free vibration condition. They adopted proper orthogonal decomposition (POD) or the so-called Karhunen Loeve decomposition (KLD) to obtain mode shape vectors only. Han and Feeny [12] applied POD to obtain proper orthogonal mode (POM) that is the structural normal mode. The practical limitation is that the mass matrix must be proportional to the identity matrix.

Feeny and Liang [13] further expanded the POD method to the discrete and continuous systems in random excitation; however, the known mass matrix in priori is its limitation. Kershen and Golinval [14] commented on Feeny and Liang's work [13] and showed that the empirical orthogonal function (EOF) of a system is the system's normal mode and is the POM indicated by Feeny and Liang[13]. Azeez and Vakakis [15] also adopted POD or KLD method to determine structural modes of beams and rotor system subject to vibration shock and used the vibration response to monitor damage in real-time. Kerschen and Golinval [16] applied POD to develop modal analysis for both undamped and damped system in free vibration and harmonic excitation and showed the feasibility using digitalized, discrete signal to get modal parameters. For the identification of mdof system modal parameters, Chakraborty et al. [17] presented a wavelet-based approach to effectively extract natural frequencies and the corresponding mode shapes from the system transient response due to ambient vibration.

This work presents the algorithm of modal analysis by using free vibration response only (MAFVRO). Section 2 briefly reviews the theoretical modal analysis (TMA) and transient response analysis for the discrete mdof system. Section 3 shows the development of MAFVRO algorithm. Sections 4 and 5 present the solution procedures and normal modes prediction results, respectively. Results show the MAFVRO algorithm is promising and potential to extend to continuous system and practical application.

2. Theoretical analysis for mdof system

Consider a mdof vibration system with proportional viscous damping. The general form of equation of motion can be expressed as follows:

$$\mathbf{M}\ddot{\mathbf{x}} + \mathbf{C}\dot{\mathbf{x}} + \mathbf{K}\mathbf{x} = \mathbf{f} \tag{1}$$

and

$$\mathbf{C} = \alpha\mathbf{M} + \beta\mathbf{K}. \tag{2}$$

The initial conditions are:

$$\mathbf{x}(0) = \mathbf{x}_0, \tag{3}$$

$$\dot{\mathbf{x}}(0) = \mathbf{v}_0. \tag{4}$$

2.1. Modal analysis

For normal mode analysis, let

$$\mathbf{x} = \mathbf{X}e^{i\omega t}. \tag{5}$$

By the substitution of Eq. (5) into Eq. (1) and the assumptions $\mathbf{f} = \mathbf{0}$ and $\mathbf{C} = \mathbf{0}$, the generalized eigenvalues problem can now be formulated:

$$\mathbf{K}\mathbf{X} = \omega^2\mathbf{M}\mathbf{X} \tag{6}$$

or

$$\mathbf{M}^{-1}\mathbf{K}\mathbf{X} = \omega^2\mathbf{X}. \tag{7}$$

By solving the above equation, n-pairs of eigenvalues ω_r^2 and eigenvector $\mathbf{X}_r$ can be obtained. The mass-matrix normalized mode shape can be determined as

$$\phi_r = \frac{1}{\sqrt{m_r}}\mathbf{X}_r, \tag{8}$$

where

$$m_r = \mathbf{X}_r^{\mathrm{T}}\mathbf{M}\mathbf{X}_r. \tag{9}$$

The orthogonality of mode shape in matrix form can be derived as follows:

$$\mathbf{\Phi}^{\mathrm{T}}\mathbf{M}\mathbf{\Phi} = \text{diag } \mathbf{I}, \tag{10}$$

$$\mathbf{\Phi}^{\mathrm{T}}C\mathbf{\Phi} = \text{diag } \mathbf{2\xi}_r\omega_r, \tag{11}$$

$$\mathbf{\Phi}^{\mathrm{T}}\mathbf{K}\mathbf{\Phi} = \text{diag } \omega_r^2, \tag{12}$$

where

$$\mathbf{\Phi} = [\phi_1, \phi_2, \ldots, \phi_n], \tag{13}$$

$$\xi_r = \frac{\alpha}{2\omega_r} + \frac{\beta\omega_r}{2}. \tag{14}$$

2.2. Free vibration analysis

The mode shape vectors, due to their property of orthogonality, are linearly independent. The system response can be expressed as follows from expansion theorem:

$$\mathbf{x}(t) = \sum_{r=1}^{n} \phi_r q_r(t) = \mathbf{\Phi}\mathbf{q}(t). \tag{15}$$

For unforced condition, i.e. $\mathbf{f}(t) = 0$, by the substitution of Eq. (15) into Eq. (1) and the employment of orthogonality relation, the n pair independent equations can be obtained:

$$\ddot{q}_r + 2\xi_r\omega_r\dot{q}_r + \omega_r^2 q_r = 0, \quad r = 1, 2, \ldots, n. \tag{16}$$

The corresponding initial conditions of modal coordinate $q_r(t)$ can be written as

$$\mathbf{q}(0) = \mathbf{q}_0 = \mathbf{\Phi}^{\mathrm{T}}\mathbf{M}\mathbf{x}_0, \tag{17}$$

$$\dot{\mathbf{q}}(0) = \dot{\mathbf{q}}_0 = \mathbf{\Phi}^{\mathrm{T}}\mathbf{M}\mathbf{v}_0. \tag{18}$$

$q_{r0} = q_r(0)$ and $\dot{q}_{r0} = \dot{q}_r(0)$ denote the initial displacement and velocity of $q_r(t)$, respectively. The free vibration response $q_r(t)$ can be determined as follows [18]:

(1) Undamped and under-damped ($0 \leqslant \xi < 1$)

$$q_r(t) = \mathrm{e}^{-\xi_r\omega_r t}\left[q_{r0} \cos \omega_{\mathrm{d}r} t + \frac{\dot{q}_{r0} + \xi_r\omega_r q_{r0}}{\omega_{\mathrm{d}r}} \sin \omega_{\mathrm{d}r} t\right], \tag{19}$$

where

$$\omega_{\mathrm{d}r} = \omega_r\sqrt{1 - \xi_r^2}. \tag{20}$$

(2) Critically damped ($\xi = 1$)

$$q_r(t) = [q_{r0} + (\dot{q}_{r0} + \omega_r q_{r0})t]\mathrm{e}^{-\omega_r t}. \tag{21}$$

(3) Overdamped ($\xi > 1$)

$$q_r(t) = \mathrm{e}^{-\xi_r \omega_r t}\left[\frac{\dot{q}_{r0} + \left(\xi_r + \sqrt{\xi_r^2 - 1}\right)\omega_r q_{r0}}{2\bar{\omega}_{\mathrm{d}r}}\mathrm{e}^{\bar{\omega}_{\mathrm{d}r} t} + \frac{-\dot{q}_{r0} - \left(\xi_r - \sqrt{\xi_r^2 - 1}\right)\omega_r q_{r0}}{2\bar{\omega}_{\mathrm{d}r}}\mathrm{e}^{-\bar{\omega}_{\mathrm{d}r} t}\right], \tag{22}$$

where

$$\bar{\omega}_{\mathrm{d}r} = \omega_r\sqrt{\xi_r^2 - 1}. \tag{23}$$

The system displacement response $\mathbf{x}(t)$ can then be obtained from Eq. (15).

3. Modal analysis from free vibration response

The intention of this work is to determine modal parameters, including natural frequencies ω_r and mode shape $\boldsymbol{\phi}_r$, from the free vibration response, i.e $\mathbf{f(t)} = 0$. For proportional viscous damping without prescribed force, the system equation becomes

$$\mathbf{M}\ddot{\mathbf{x}} + (\alpha\mathbf{M} + \beta\mathbf{K})\dot{\mathbf{x}} + \mathbf{K}\mathbf{x} = 0. \tag{24}$$

Rearrange the above equation

$$\mathbf{M}(\ddot{\mathbf{x}} + \alpha\dot{\mathbf{x}}) = -\mathbf{K}(\mathbf{x} + \beta\dot{\mathbf{x}}). \tag{25}$$

Then

$$\mathbf{M}^{-1}\mathbf{K} = -(\ddot{\mathbf{x}} + \alpha\dot{\mathbf{x}})(\mathbf{x} + \beta\dot{\mathbf{x}})^{-1}. \tag{26}$$

By comparing Eqs. (26) and (7), one can conclude that if the system response $\mathbf{x}$, $\dot{\mathbf{x}}$ and $\ddot{\mathbf{x}}$ are known, $\mathbf{M}^{-1}\mathbf{K}$ can be formulated and used to solve the eigenvalues and eigenvectors, i.e. the normal modes of the system. Consider the system displacement response matrix as follows:

$$\mathbf{X} = [X]_{N_k \times n} = \begin{bmatrix} x_{1,k} & x_{2,k} & \cdots & x_{n,k} \\ x_{1,k+1} & x_{2,k+1} & \cdots & x_{n,k+1} \\ \vdots & \vdots & \ddots & \vdots \\ x_{1,k+N_k-1} & x_{2,k+N_k-1} & \cdots & x_{n,k+N_k-1} \end{bmatrix} = \left[\begin{Bmatrix} x_{1,k} \\ x_{2,k} \\ \vdots \\ x_{n,k} \end{Bmatrix}\begin{Bmatrix} x_{1,k+1} \\ x_{2,k+1} \\ \vdots \\ x_{n,k+1} \end{Bmatrix}\cdots\begin{Bmatrix} x_{1,k+N_k-1} \\ x_{2,k+N_k-1} \\ \vdots \\ x_{n,k+N_k-1} \end{Bmatrix}\right]^{\mathrm{T}}$$
$$= \left[\{x\}_k\{x\}_{k+1}\cdots\{x\}_{k+N_k-1}\right]^{\mathrm{T}}, \tag{27}$$

where $x_{r,k} = x_r(t_k)$ denotes the displacement of the rth dof at time t_k. Similarly, the system velocity and acceleration response matrix can be defined:

$$\dot{\mathbf{X}} = [\dot{X}] = [\{\dot{x}\}_k\{\dot{x}\}_{k+1}\ldots\{\dot{x}\}_{k+N_k-1}]^{\mathrm{T}}, \tag{28}$$

$$\ddot{\mathbf{X}} = [\ddot{X}] = [\{\ddot{x}\}_k\{\ddot{x}\}_{k+1}\ldots\{\ddot{x}\}_{k+N_k-1}]^{\mathrm{T}}. \tag{29}$$

Eq. (26) can then be rewritten as follows:

$$\mathbf{M}^{-1}\mathbf{K} = -(\ddot{\mathbf{X}}^{\mathrm{T}} + \alpha\dot{\mathbf{X}}^{\mathrm{T}})(\beta\dot{\mathbf{X}}^{\mathrm{T}} + \mathbf{X}^{\mathrm{T}})^{-1}. \tag{30}$$

If the displacement sensor is used to measure the system displacement response, $x_r(t_k) = x_{r,k}$, as illustrated in Fig. 1, the velocity and acceleration can be determined by finite-difference method. Table 1 shows the

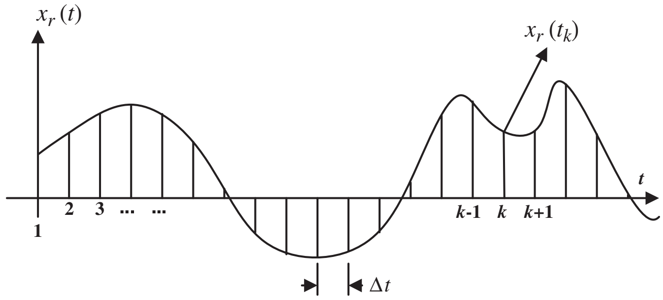

Fig. 1. Discrete displacement response in time domain.

Table 1
Formula to evaluate the velocity and acceleration

Method	Velocity	Acceleration
First-order backward formula	$v_{r,k} = \dot{x}_{r,k} = \frac{1}{\Delta t}(x_{r,k} - x_{r,k-1})$	$a_{r,k} = \ddot{x}_{r,k} = \frac{1}{\Delta t}(v_{r,k} - v_{r,k-1})$
Second-order backward formula	$v_{r,k} = \dot{x}_{r,k} = \frac{1}{\Delta t}(3x_{r,k} - 4x_{r,k-1} + x_{r,k-2})$	$a_{r,k} = \ddot{x}_{r,k} = \frac{1}{\Delta t}(3v_{r,k} - 4v_{r,k-1} + v_{r,k-2})$
First central formula	$v_{r,k} = \dot{x}_{r,k} = \frac{1}{2\Delta t}(x_{r,k+1} - x_{r,k-1})$	$a_{r,k} = \ddot{x}_{r,k} = \frac{1}{2\Delta t}(v_{r,k+1} - v_{r,k-1})$
Second central formula	$v_{r,k} = \dot{x}_{r,k} = \frac{1}{12\Delta t}(-x_{r,k+2} + 8x_{r,k+1} - 8x_{r,k-1} + x_{r,k-2})$	$a_{r,k} = \ddot{x}_{r,k} = \frac{1}{12\Delta t}(-v_{r,k+2} + 8v_{r,k+1} - 8v_{r,k-1} + v_{r,k-2})$

formula to evaluate the velocity and acceleration. For the first-order central formula, let $n = 2$, $N_k = 3$ to illustrate the derivation of velocity and acceleration response matrices:

$$\dot{\mathbf{X}} = [\dot{X}] = \begin{bmatrix} v_{1,k-1} & v_{2,k-1} \\ v_{1,k} & v_{2,k} \\ v_{1,k+1} & v_{2,k+1} \\ v_{1,k+2} & v_{2,k+2} \\ v_{1,k+3} & v_{2,k+3} \end{bmatrix} = \frac{1}{2\Delta t} \begin{bmatrix} -1 & 0 & 1 & 0 & 0 & 0 & 0 \\ 0 & -1 & 0 & 1 & 0 & 0 & 0 \\ 0 & 0 & -1 & 0 & 1 & 0 & 0 \\ 0 & 0 & 0 & -1 & 0 & 1 & 0 \\ 0 & 0 & 0 & 0 & -1 & 0 & 1 \end{bmatrix} \begin{bmatrix} x_{1,k-2} & x_{2,k-2} \\ x_{1,k-1} & x_{2,k-1} \\ x_{1,k} & x_{2,k} \\ x_{1,k+1} & x_{2,k+1} \\ x_{1,k+2} & x_{2,k+2} \\ x_{1,k+3} & x_{2,k+3} \\ x_{1,k+4} & x_{2,k+4} \end{bmatrix}, \tag{31}$$

$$\dot{\mathbf{X}} = \mathbf{D}_1 \mathbf{X}, \tag{32}$$

$$\ddot{X} = \left[\ddot{X}\right] = \begin{bmatrix} a_{1,k} & a_{2,k} \\ a_{1,k+1} & a_{2,k+1} \\ a_{1,k+2} & a_{2,k+2} \end{bmatrix} = \frac{1}{2\Delta t} \begin{bmatrix} -1 & 0 & 1 & 0 & 0 \\ 0 & -1 & 0 & 1 & 0 \\ 0 & 0 & -1 & 0 & 1 \end{bmatrix} \begin{bmatrix} v_{1,k-1} & v_{2,k-1} \\ v_{1,k} & v_{2,k} \\ v_{1,k+1} & v_{2,k+1} \\ v_{1,k+2} & v_{2,k+2} \\ v_{1,k+3} & v_{2,k+3} \end{bmatrix}, \tag{33}$$

$$\ddot{\mathbf{X}} = \mathbf{D}_2 \dot{\mathbf{X}}, \tag{34}$$

where

$$\mathbf{D}_1 = [D_1] = \frac{1}{2\Delta t}\begin{bmatrix} -1 & 0 & 1 & 0 & 0 & 0 & 0 \\ 0 & -1 & 0 & 1 & 0 & 0 & 0 \\ 0 & 0 & -1 & 0 & 1 & 0 & 0 \\ 0 & 0 & 0 & -1 & 0 & 1 & 0 \\ 0 & 0 & 0 & 0 & -1 & 0 & 1 \end{bmatrix}, \tag{35}$$

$$\mathbf{D}_2 = [D_2] = \frac{1}{2\Delta t}\begin{bmatrix} -1 & 0 & 1 & 0 & 0 \\ 0 & -1 & 0 & 1 & 0 \\ 0 & 0 & -1 & 0 & 1 \end{bmatrix}. \tag{36}$$

For other finite difference methods, one can derive similar equations for $\mathbf{D}_1$ and $\mathbf{D}_2$ omitted here for brevity. And, the effect of different finite difference methods on the prediction accuracy of modal parameters for the developed algorithm is presented in Section 5. It is noted that if the system displacement response $x_r(t_k)$ can be measured and discreteized to formulate the displacement response matrix as shown in Eq. (27), velocity and acceleration response matrices can then be determined by Eqs. (32) and (34). The matrix $\mathbf{M}^{-1}\mathbf{K}$ can be obtained through Eq. (30) and solved for the eigenvalue ω_r^2 and eigenvectors $\mathbf{X}_r$ as derived in Eq. (7). In contrast to Zhou and Chelidze's approach [10] by SOD method, the derivation of current approach is straightforward and physically interpreted. The extension of the method to general or non-proportional damping mdof system or even continuous system is feasible. The merit of the developed algorithm is that only the time domain data of free vibration response is required to measure, and the numerical calculation is simple and easy to be implemented.

4. Development of MAFVRO

This section briefly introduces the development of MATLAB program to perform Modal Analysis by using Free Vibration Response Only (MAFVRO). The solution flow chart is shown in Fig. 2 and discussed as follows:

1. Define the system matrix $\mathbf{M}$, $\mathbf{C}$ and $\mathbf{K}$, in which $\mathbf{C} = \alpha\mathbf{M} + \beta\mathbf{K}$.
2. Define the initial condition vectors $\mathbf{x}_0$, $\mathbf{v}_0$ for each dof.
3. Perform theoretical modal analysis to find exact solutions of natural frequencies ω_r and its corresponding mode shape vector ϕ_r.
4. Determine the transient-free vibration response $\mathbf{x}(t)$ due to the initial condition and use the exact solution of $\mathbf{x}(t)$ as the measured response. In practical application, $\mathbf{x}(t)$ is measured by real experiments to collect the time series displacement response.
5. Include noise signal into the transient displacement response by employing MATLAB function "randn" to generate random number as follows:
$$x_r(t_k) = \mathrm{MAX}(|x_r(t_k)|)\bullet\mathrm{SNR}\bullet\mathrm{RAN} + x_r(t_k), \tag{37}$$
where RAN is the normally distributed random number between -1 and 1; SNR is the percentage of signal-to-noise ratio; $\mathrm{MAX}(|x_r(t_k)|)$ is the maximum displacement in simulation.
6. Formulate the displacement response matrix and apply finite difference method to determine the velocity and acceleration response matrices, respectively.
7. Employ Eq. (30) to solve an eigenvalue problem and obtain modal parameters $\hat{\omega}_r$, $\hat{\phi}_r$ by MAFVRO method.
8. Compare the prediction results with the theoretical ones. Natural frequencies are shown in the percentage of prediction error defined as follows:
$$\varepsilon_r = \frac{(\hat{f}_r - f_r)}{f_r} \times 100\% \tag{38}$$

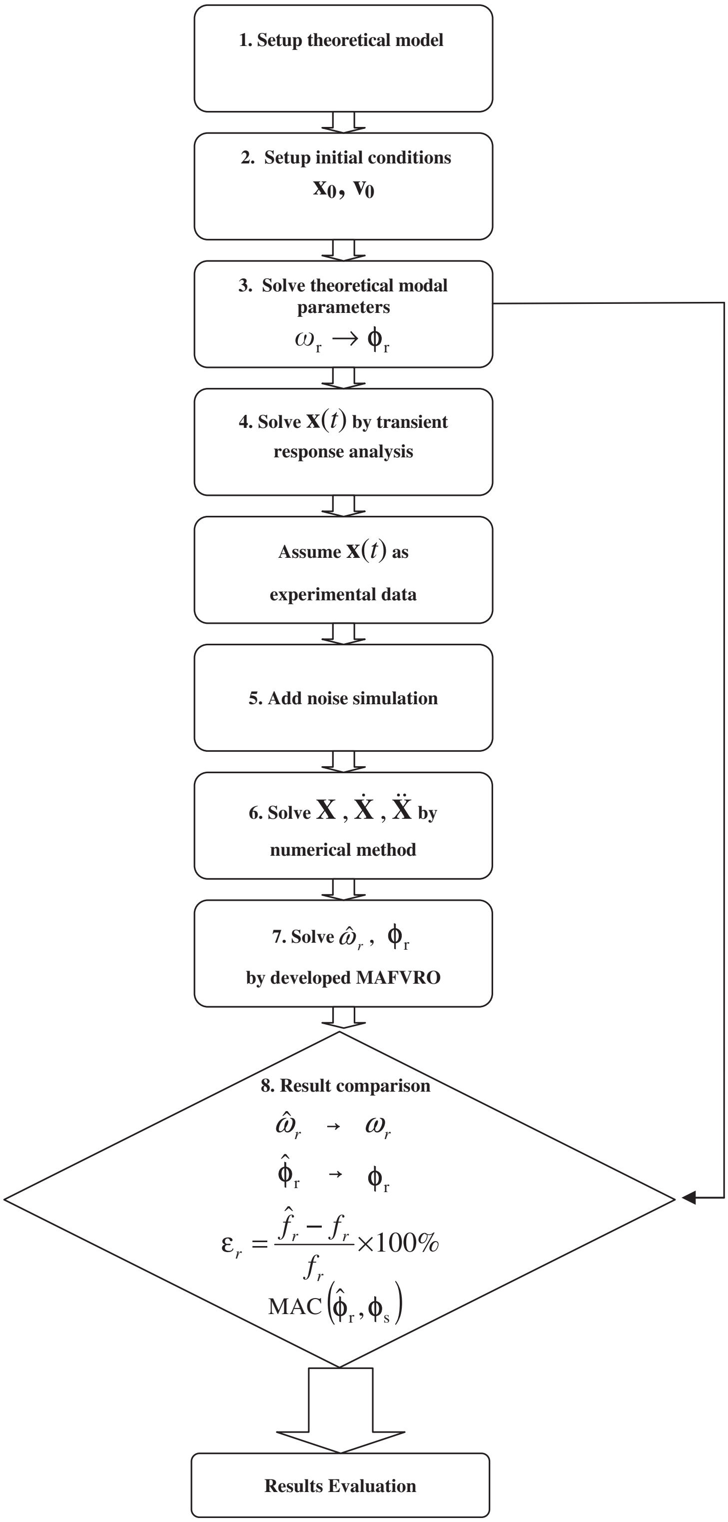

Fig. 2. Solution flow chart for MAFVRO program.

and mode shape vectors are evaluated by Modal Assurance Criterion (MAC) as follows:

$$\mathrm{MAC}\left(\hat{\phi}_r, \phi_s\right) = \frac{|\hat{\phi}_r^{\mathrm{T}} \phi_s|^2}{\left(\hat{\phi}_r^{\mathrm{T}} \hat{\phi}_r^*\right)\left(\phi_s^{\mathrm{T}} \phi_s^*\right)}, \quad r = 1, 2, \ldots, n, \quad s = 1, 2, \ldots, n. \tag{39}$$

If the diagonal terms of MAC matrix are one, the compared two mode shape vectors are exactly the same modes even if they are not in the same scale. If the off-diagonal terms are zero, the two mode shape vectors are orthogonal. MAC is generally used to justify the quality of experimental mode shape in comparison to the theoretical one. In this work, MAC is used to evaluate the correctness of the predicted mode shape vectors.

It is noted that several program parameters must be properly set up to complete the solution and discussed as follows:

1. The sampling frequency f_s or discrete time interval (Δt) needs to be defined so as to discretize the system response and is an important variable in real experiment:

$$f_s = \frac{1}{\Delta t}. \tag{40}$$

2. Number of data points (N_t) in transient response simulation is specified to emulate the practical experimental measurement.
3. The started number of data point (k) as well as the number of data points (N_k) for the MAFVRO algorithm is defined to formulate the response matrices.
4. The noise variable (SNR) is specified up to 10% to test the accommodation of MAFVRO algorithm to noise effects.
5. The optimal parameters will be tested and discussed in the next section.

5. Results and discussions

This section presents the simulation results by using MAFVRO algorithm to extract system modal parameters by using free vibration response data only. Different n-dof systems are, respectively, chosen and shown in Fig. 3 to simulate the modal analysis by the developed algorithm. Table 2 summarizes the system parameters for mdof systems. Only the unity initial displacement vector is prescribed for simulation of free vibration.

5.1. Effect of algorithm parameters

The first algorithm parameter to show is the number of data point N_k that are used to construct system response matrices. The sampling frequency is set to $f_s = 6000$ Hz, and the started data point is $k = 3$.

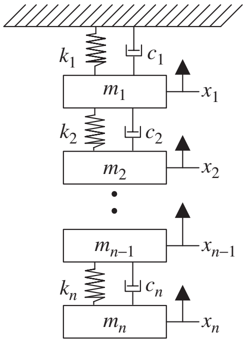

Fig. 3. n dof system model.

Table 2
System parameters for mdof system

System	10 dofs
M	$\begin{bmatrix} m_1 & 0 & 0 & \cdots & 0 \\ 0 & m_2 & 0 & \ldots & 0 \\ 0 & 0 & m_3 & \ddots & \vdots \\ \vdots & \vdots & \ddots & \ddots & 0 \\ 0 & 0 & \cdots & 0 & m_n \end{bmatrix}_{n\times n}$
K	$\begin{bmatrix} (k_1+k_2) & -k_2 & \cdots & 0 & 0 \\ -k_2 & (k_2+k_3) & \cdots & 0 & 0 \\ \vdots & \vdots & \ddots & \ddots & \vdots \\ \vdots & \vdots & \ddots & (k_{n-1}+k_n) & -k_n \\ 0 & 0 & \cdots & -k_n & k_n \end{bmatrix}_{n\times n}$
I.C.	$\mathbf{x}_0^\mathrm{T} = [1; 1; \ldots; 1]_{n\times 1}$ $\mathbf{v}_0^\mathrm{T} = [0; 0; \ldots; 0]_{n\times 1}$

Note: $k_i = 1{,}000{,}000\,\mathrm{N\,m^{-1}}$, $m_i = 1\,\mathrm{kg}$, $i = 1, 2,\ldots,n$.

Table 3
Natural frequency prediction errors (%)for different numbers of data points

N_k	ε_1	ε_2	ε_3	ε_4	ε_5	ε_6	ε_7	ε_8	ε_9	ε_{10}
50	−0.0103	−0.0917	−0.2470	−0.4623	−0.7183	−0.9922	−1.2594	−1.4965	−1.6824	−1.8009
100	−0.0103	−0.0917	−0.2470	−0.4623	−0.7183	−0.9922	−1.2594	−1.4965	−1.6824	−1.8009
150	−0.0103	−0.0917	−0.2470	−0.4623	−0.7183	−0.9922	−1.2594	−1.4965	−1.6824	−1.8009
200	−0.0103	−0.0917	−0.2470	−0.4623	−0.7183	−0.9922	−1.2594	−1.4965	−1.6824	−1.8009
250	−0.0103	−0.0917	−0.2470	−0.4623	−0.7183	−0.9922	−1.2594	−1.4965	−1.6824	−1.8009

Note: $f_s = 6000\,\mathrm{Hz}$, $k = 3$, SNR = 0.

Table 4
Natural frequency prediction errors (%) for different started number of data points

k	ε_1	ε_2	ε_3	ε_4	ε_5	ε_6	ε_7	ε_8	ε_9	ε_{10}
3	−0.0103	−0.0917	−0.2470	−0.4623	−0.7183	−0.9922	−1.2594	−1.4965	−1.6824	−1.8009
300	−0.0103	−0.0917	−0.2470	−0.4623	−0.7183	−0.9922	−1.2594	−1.4965	−1.6824	−1.8009
500	−0.0103	−0.0917	−0.2470	−0.4623	−0.7183	−0.9922	−1.2594	−1.4965	−1.6824	−1.8009

Note: $f_s = 6000\,\mathrm{Hz}$, $N_k = 50$, SNR = 0.

In this paper, without further notes the first-order central formula is employed to formulate the response matrices, and noise effect is not included. Table 3 shows the prediction error for the natural frequencies of the 10-dof system. N_k is ranged from 50 to 250. The prediction error is no more than 2% for the highest natural frequency $f_{10} = 314.7546\,\mathrm{Hz}$ and different range of data points reveals the same prediction results.

The next test is to choose different started numbers $k = 3$, 300, 500 as shown in Table 4, while $f_s = 6000\,\mathrm{Hz}$ and $N_k = 50$. The prediction errors are almost the same as those in Table 3. From the above, this indicates that only a few data points ($N_k = 50$) are required and make the algorithm efficiency. It is flexible to choose any range of data points resulting in good prediction.

Table 5
Natural frequency prediction errors (%) for different sampling frequency

f_s (Hz)	f_s/f_{10}	ε_1	ε_2	ε_3	ε_4	ε_5	ε_6	ε_7	ε_8	ε_9	ε_{10}	Avgd error	Max error	Min error
500	1.59	−45.5919	−76.6473	−79.8484	−77.7004	−75.8095	−78.5371	−78.0071	−78.4364	−76.2107	−74.8688	−74.1658	−79.8484	−45.5919
1000	3.18	−0.3719	−3.2685	−8.6637	−15.8529	−26.3528	−35.7045	−42.6299	−45.9801	−47.9619	−49.6038	−27.639	−49.6038	−0.3719
1200	3.81	−0.2583	−2.2767	−6.0658	−11.1788	−17.0501	−23.0859	−28.7403	−33.6037	−37.3606	−39.3367	−19.8957	−39.3367	−0.2583
1500	4.77	−0.1654	−1.4607	−3.9081	−7.2445	−11.1267	−15.1785	−19.0347	−22.3747	−24.9424	−26.5552	−13.1991	−26.5552	−0.1654
2000	6.35	−0.0931	−0.8232	−2.2098	−4.1149	−6.3542	−8.7185	−10.9957	−12.9905	−14.5388	−15.5180	−7.63567	−15.518	−0.0931
2500	7.94	−0.0596	−0.5273	−1.4177	−2.6454	−4.0953	−5.6341	−7.1244	−8.4365	−9.4593	−10.1082	−4.95078	−10.1082	−0.0596
5000	**15.89**	**−0.0149**	**−0.1320**	**−0.3556**	**−0.6653**	**−1.0334**	**−1.4268**	**−1.8105**	**−2.1506**	**−2.4173**	**−2.5871**	**−1.25935**	**−2.5871**	**−0.0149**
6000	**19.06**	**−0.0103**	**−0.0917**	**−0.2470**	**−0.4623**	**−0.7183**	**−0.9922**	**−1.2594**	**−1.4965**	**−1.6824**	**−1.8009**	**−0.8761**	**−1.8009**	**−0.0103**
8192	**26.03**	**−0.0055**	**−0.0492**	**−0.1325**	**−0.2482**	**−0.3857**	**−0.5330**	**−0.6768**	**−0.8044**	**−0.9046**	**−0.9685**	**−0.47084**	**−0.9685**	**−0.0055**

Note: $N_k = 50$, $k = 3$, SNR $= 0$.

It is also of interest to study the effect of sampling frequency. Table 5 shows the prediction errors of natural frequencies for a 10-dof system by using different sampling frequencies. As the increase of sampling frequency, the prediction errors of natural frequencies decrease significantly. The maximum errors are within $\pm 3\%$ for $f_s = 5000\,\text{Hz}$, $\pm 2\%$ for $f_s = 6000\,\text{Hz}$, and $\pm 1\%$ for $f_s = 8192\,\text{Hz}$, respectively. The frequency ratios $f_s/\max(f_n)$ are about 15.92, 19.06 and 26.09, respectively.

The above results are based on the first-order central formula to obtain the system response matrices so as to perform modal parameter identification. Table 1 summarizes four kinds of finite different methods that can be adopted to determine the velocity and acceleration response matrices as discussed in Section 3. Table 6 shows the prediction errors of natural frequencies for a 6-dof system by using different finite difference formula. Different formula results in different sampling frequencies for the predicted natural frequency errors within $\pm 2\%$. The second-order central formula reveals the best results and requires $f_s = 2500\,\text{Hz}$ about 8 times of the highest natural frequency ($f_s/f_6 = 8.089$).

Finally, for studying the accommodation of MAFVRO algorithm to signal noise, the SNR is set to different values according to Eq. (37). Table 7 shows the prediction results of a 3-dof system for different SNR values by using different finite difference methods. From Table 7 the natural frequency prediction errors within $\pm 2\%$ are set in, and one can observe that the second-order central formula is the best choice and can accommodate up to SNR = 10%. The MAC matrix close to a unity matrix indicates the predictions of mode shape vector are also very well. That diagonal MAC values are close to 1 indicates the mode shape vectors prediction is nearly the same. And, off-diagonal MAC values close to 0 means the predicted mode shapes are truly orthogonal. The adoption of more sophisticated finite difference formula in determining the velocity and acceleration matrices can provide more accuracy in predicting the modal parameters. The second-order central formula can be sufficient for practical application.

5.2. Effect of system parameters

In this section, different system parameters are studied. Table 8 shows the prediction results for the 3-dof and 10-dof systems, for $N_k = 50$, $k = 3$, $f_s = 6000\,\text{Hz}$, $\alpha = 0.001$, $\beta = 0.001$ and SNR = 0. The natural

Table 6
Natural frequency prediction errors (%) for different finite difference formula

Finite difference method	f_s	f_s/f_6	ε_1	ε_2	ε_3	ε_4	ε_5	ε_6	Avgd error	Max error	Min error
First-order backward formula	4000	12.942	0.005	−1.002	−2.379	−3.367	−5.254	−7.920	−3.320	−7.920	0.005
	5000	16.178	−0.113	−0.580	−1.649	−2.204	−4.494	−3.989	−2.171	−4.494	−0.113
	6000	19.414	−0.192	−0.201	−0.983	−0.792	−3.356	−2.905	−1.405	−3.356	−0.192
	7000	22.649	−0.137	−0.507	−0.725	−1.707	−1.887	−2.192	−1.193	−2.192	−0.137
	7500	**24.267**	**−0.037**	**−0.307**	**−0.639**	**−1.347**	**−1.841**	**−1.305**	**−0.913**	**−1.841**	**−0.037**
Second-order backward formula	5000	16.178	0.077	0.666	1.686	2.901	3.978	4.820	2.355	4.820	0.077
	6000	19.414	0.054	0.465	1.182	2.051	2.799	3.391	1.657	3.391	0.054
	7000	22.649	0.039	0.340	0.870	1.496	2.089	2.510	1.224	2.510	0.039
	7500	24.267	0.034	0.297	0.759	1.309	1.815	2.218	1.072	2.218	0.034
	8000	**25.885**	**0.030**	**0.261**	**0.668**	**1.154**	**1.591**	**1.951**	**0.943**	**1.951**	**0.030**
First-order central formula	2000	6.471	−0.242	−2.083	−5.292	−9.080	−12.566	−14.981	−7.374	−14.981	−0.242
	3000	9.707	−0.108	−0.929	−2.373	−4.099	−5.705	−6.838	−3.342	−6.838	−0.108
	4000	12.942	−0.061	−0.523	−1.339	−2.318	−3.234	−3.883	−1.893	−3.883	−0.061
	5000	16.178	−0.039	−0.335	−0.858	−1.487	−2.078	−2.494	−1.215	−2.494	−0.039
	6000	**19.414**	**−0.027**	**−0.233**	**−0.596**	**−1.034**	**−1.446**	**−1.736**	**−0.845**	**−1.736**	**−0.027**
Second-order central formula	1000	3.236	−0.011	−0.794	−4.762	−12.810	−23.461	−29.360	−11.866	−29.360	−0.011
	1500	4.853	−0.002	−0.162	−1.025	−2.937	−5.481	−7.666	−2.879	−7.666	−0.002
	2000	6.471	−0.001	−0.052	−0.334	−0.979	−1.867	−2.644	−0.979	−2.644	−0.001
	2500	**8.089**	**0.000**	**−0.021**	**−0.139**	**−0.410**	**−0.790**	**−1.129**	**-0.415**	**-1.129**	**0.000**

Note: $N_k = 200$, $k = 50$, SNR = 0.

Table 7
Noise effect on prediction results for different finite difference formula

Method	SNR (%)	Predicted $\hat{f}_r$ (Hz)			Predicted error (%)			$\mathrm{MAC}\left(\hat{\phi}_r, \phi_s\right)$		
		$\hat{f}_1$	$\hat{f}_2$	$\hat{f}_3$	ε_1	ε_2	ε_3			
First-order backward formula	0.5	69.712	200.080	282.600	−1.580	0.817	−1.460	**0.99992**	0.00007	0.00001
								0.00133	**0.99865**	0.00003
								0.00117	0.00487	**0.99396**
	1	70.108	200.130	283.470	−1.020	0.840	−1.155	**0.99974**	0.00025	0.00001
								0.00190	**0.99727**	0.00083
								0.00436	0.00018	**0.99546**
	1.1	70.539	200.600	281.810	−0.411	1.076	−1.737	**1.00000**	0.00000	0.00000
								0.00030	**0.99820**	0.00150
								0.00060	0.02610	**0.97330**
	1.2	**69.746**	**201.080**	**280.870**	**−1.532**	**1.318**	**−2.065**	**0.99980**	0.00020	0.00000
								0.00310	**0.99570**	0.00120
								0.00670	0.00800	**0.98530**
Second-order backward formula	0.1	71.154	202.930	295.740	0.456	2.249	3.123	**0.99997**	0.00003	0.00001
								0.00006	**0.99962**	0.00032
								0.00015	0.00741	**0.99244**
	0.2	70.084	196.700	288.530	−1.054	−0.890	0.607	**0.99990**	0.00010	0.00000
								0.00110	**0.99860**	0.00030
								0.00200	0.01500	**0.98300**
	0.3	69.592	196.990	288.810	−1.749	−0.740	0.705	**1.00000**	0.00000	0.00000
								0.00000	**1.00000**	0.00000
								0.00000	0.00350	**0.99640**
	0.32	**69.439**	**201.220**	**286.300**	**−1.964**	**1.388**	**−0.171**	**1.00000**	0.00000	0.00000
								0.00010	**0.99960**	0.00030
								0.00000	0.00250	**0.99750**
First-order central formula	0.01	70.757	197.055	282.554	−0.029	−0.701	−1.482	**1.00000**	0.00000	0.00000
								0.00000	**1.00000**	0.00000
								0.00000	0.00000	**1.00000**
	0.1	70.895	196.953	282.586	−1.252	−0.755	−1.452	**1.00000**	0.00000	0.00000
								0.00000	**1.00000**	0.00000
								0.00000	0.00000	**1.00000**
	1	72.036	198.028	284.611	1.701	−0.219	−0.759	**0.99970**	0.00000	0.00030
								0.00010	**0.99980**	0.00000
								0.00000	0.00010	**0.99990**
	3	**71.994**	**198.610**	**292.350**	**1.642**	**0.072**	**1.940**	**1.00000**	0.00000	0.00000
								0.00010	**0.99970**	0.00020
								0.00030	0.00000	**0.99970**
Second-order central formula	1	70.852	197.790	283.320	0.031	−0.342	−1.208	**1.00000**	0.00000	0.00000
								0.00001	**0.99999**	0.00001
								0.00001	0.00000	**0.99999**
	3	70.742	198.320	284.540	−0.125	−0.073	−0.783	**1.00000**	0.00000	0.00000
								0.00002	**0.99997**	0.00000
								0.00013	0.00041	**0.99945**
	5	71.290	198.620	284.890	0.649	0.078	−0.660	**0.99999**	0.00001	0.00000
								0.00007	**0.99972**	0.00020
								0.00061	0.00065	**0.99874**
	10	**71.887**	**201.860**	**291.780**	**1.492**	**1.710**	**1.739**	**0.99991**	0.00000	0.00009
								0.00060	**0.99931**	0.00009
								0.00709	0.01727	**0.97564**

Note: $N_k = 50$, $k = 20$.

Table 8
Prediction results for different dofs system

(a) 3-dof system

Mode		1	2	3
f_r	TMA	70.8306	198.4630	286.7873
	MAFVRO	70.7657	197.0373	282.4956
	Error%	−0.0917	−0.7183	−1.4965
ξ_r		0.003542	0.009924	0.01434
MAC value		**1.0000**	0.0000	0.0000
		0.0000	**1.0000**	0.0000
		0.0000	0.0000	**1.0000**
MAC plot	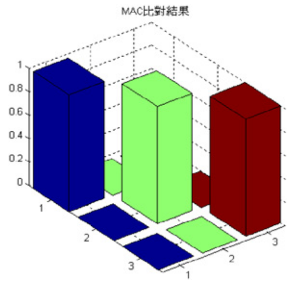			

(b) 10-dof system

Mode		1	2	3	4	5	6	7	8	9	10
f_r	TMA (Hz)	23.7873	70.8306	116.2917	159.1549	198.4630	233.3377	263.0000	286.7873	304.1683	314.7546
	MAFVRO (Hz)	23.7849	70.7657	116.0049	158.4146	197.0663	230.8960	260.1084	281.6086	300.2743	308.4068
	Error%	−0.0103	−0.0917	−0.2466	−0.4652	−0.7037	−1.0464	−1.0994	−1.8058	−1.2802	−2.0168
ξ_r		0.001191	0.003542	0.005815	0.007958	0.009923	0.011667	0.01315	0.01434	0.015209	0.015738
MAC value		**1.0000**	0.0000	0.0000	0.0000	0.0000	0.0000	0.0000	0.0000	0.0000	0.0000
		0.0000	**1.0000**	0.0000	0.0000	0.0000	0.0000	0.0000	0.0000	0.0000	0.0000
		0.0000	0.0000	**1.0000**	0.0000	0.0000	0.0000	0.0000	0.0000	0.0000	0.0000
		0.0000	0.0000	0.0000	**1.0000**	0.0000	0.0000	0.0000	0.0000	0.0000	0.0000
		0.0000	0.0000	0.0000	0.0000	**1.0000**	0.0000	0.0000	0.0000	0.0000	0.0000
		0.0000	0.0000	0.0000	0.0000	0.0000	**0.9999**	0.0001	0.0000	0.0000	0.0000
		0.0000	0.0000	0.0000	0.0000	0.0000	0.0001	**0.9990**	0.0006	0.0002	0.0001
		0.0000	0.0000	0.0000	0.0000	0.0000	0.0001	0.0009	**0.9958**	0.0027	0.0005
		0.0000	0.0000	0.0000	0.0000	0.0000	0.0001	0.0005	0.0043	**0.9867**	0.0085
		0.0000	0.0000	0.0000	0.0000	0.0000	0.0000	0.0002	0.0014	0.0116	**0.9868**
MAC plot											

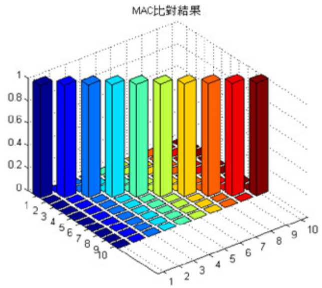

Note: $N_k = 50$, $k = 3$, $f_s = 6000\,\text{Hz}$, SNR $= 0$.

frequency prediction errors are normally within 2%. The diagonal MAC values close to 1 indicate the prediction of mode shapes is very well. Table 9 shows the prediction results for different initial conditions. Except the third modal frequency having -1.49% errors, the errors are within 1% for other modes. The MAC also reveals very good prediction for diagonal values close to 1.

Table 10 shows the prediction results of different damping ratios for underdamped and overdamped cases. The natural frequency prediction errors are about the same level for all cases within $\pm 2\%$, except a few modal frequencies within 5%. Diagonal MAC values close to 1 indicate good prediction of mode shape vectors. In summary, the developed MAFVRO algorithm shows promising for various types of mdof system

Table 9
Prediction results of 3-dof system for different initial conditions

Initial displacement vector $\mathbf{x}_0^{\mathrm{T}}$	Initial velocity vector $\mathbf{v}_0^{\mathrm{T}}$	f_r TMA (Hz)	$\hat{f}_r$ MAFVRO (Hz)	ε_r error%	MAC plot	MAC value
[5,2,8]	[0, 0, 0]	70.8306 198.4630 286.7873	70.7657 197.0373 282.4956	−0.0917 −0.7183 −1.4965	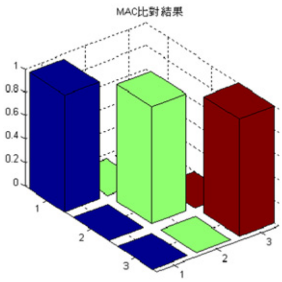	**1.0000** 0.0000 0.0000 0.0000 **1.0000** 0.0000 0.0000 0.0000 **1.0000**
[0, 0, 0]	[3,7,8]	70.8306 198.4630 286.7873	70.7657 197.0373 282.4956	−0.0917 −0.7183 −1.4965	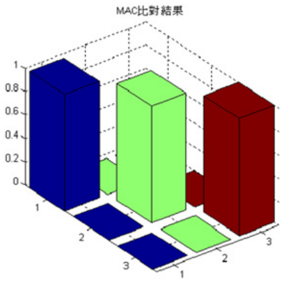	**1.0000** 0.0000 0.0000 0.0000 **1.0000** 0.0000 0.0000 0.0000 **1.0000**
[3,2,5]	[2,3,5]	70.8306 198.4630 286.7873	70.7657 197.0373 282.4956	−0.0917 −0.7183 −1.4965	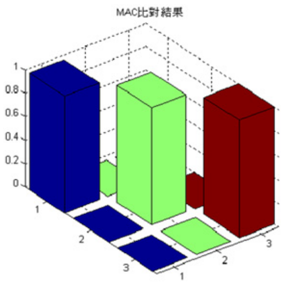	**1.0000** 0.0000 0.0000 0.0000 **1.0000** 0.0000 0.0000 0.0000 **1.0000**
[−2, −3, 7]	[−1, 5, −8]	70.8306 198.4630 286.7873	70.7657 197.0373 282.4956	−0.0917 −0.7183 −1.4965	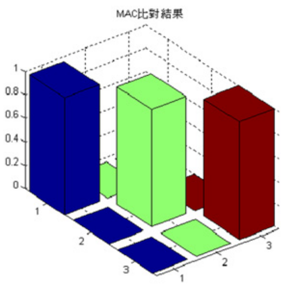	**1.0000** 0.0000 0.0000 0.0000 **1.0000** 0.0000 0.0000 0.0000 **1.0000**

Note: $N_k = 50$, $k = 3$, $f_s = 6000\,\mathrm{Hz}$, SNR = 0.

Table 10
Prediction results for different damping ratios

Type of damping	α	β	Damping ratio			MAFVRO method			Error (%)			Diagonal MAC value for each case		
			ξ_1	ξ_2	ξ_3	$\hat{f}_1$	$\hat{f}_2$	$\hat{f}_3$	ε_1	ε_2	ε_3	$\mathrm{MAC}(\hat{\phi}_1, \phi_1)$	$\mathrm{MAC}(\hat{\phi}_2, \phi_2)$	$\mathrm{MAC}(\hat{\phi}_3, \phi_3)$
Under-damped	0.0001	0.0001	0.0223	0.0624	0.0901	70.7657	70.7657	282.5475	−0.0916	−0.7125	−1.4784	0.9999	0.9995	0.9999
	500	0.0002	0.6063	0.3252	0.3189	70.8460	70.8460	282.6167	0.0263	−0.2214	−1.4917	0.9999	0.9995	0.9999
	700	0.00002	0.7910	0.2931	0.2123	70.8609	70.8609	282.7321	0.0427	−0.2095	−1.4140	0.9999	0.9995	0.9999
	1	0.0008	0.1791	0.4992	0.7207	70.7695	70.7695	282.3534	−0.0863	−0.0683	−1.5461	0.9999	0.9995	0.9999
	0.0000001	0.00005	0.0111	0.0312	0.0450	70.7657	70.7657	282.5109	−0.0916	−0.7171	−1.4911	0.9999	0.9995	0.9999
Over-damped	710	0.0011588	1.0556	1.0072	1.2406	70.8680	70.8680	292.5362	0.0528	1.1779	2.0046	1.0000	0.9999	0.9999
	600	0.001500005	1.0079	1.1758	1.5173	70.8767	70.8767	300.0767	0.0651	1.5070	4.6339	1.0000	0.9999	0.9999
	1000	0.00098	1.3416	1.0120	1.1601	70.8450	70.8450	292.3860	0.0204	0.9902	1.9522	1.0000	0.9999	0.9999
	800	0.00118	1.1614	1.0565	1.2847	70.8593	70.8593	294.5061	0.0405	1.2054	2.6915	1.0000	0.9999	0.9999
	1200	0.001	1.5708	1.1047	1.2336	70.8309	70.8309	296.5008	0.0004	0.6449	3.3870	1.0000	0.9999	0.9999
	800	0.005	2.0114	3.4383	4.7246	70.8330	70.8330	288.6401	0.0033	0.1984	0.6461	1.0000	1.0000	1.0000
	3700	0.01	6.3823	7.7186	10.0322	70.8009	70.8009	293.5298	−0.0419	1.6295	2.3511	1.0000	1.0000	1.0000
	500	0.008	2.3418	5.1885	7.3428	70.8353	70.8353	291.1682	0.0067	0.4395	1.5276	1.0000	1.0000	1.0000
	0.002	0.05	11.1250	31.1750	45.0250	70.8322	70.8322	288.5380	0.0023	0.1397	0.6105	1.0000	1.0000	1.0000
	20	0.2	44.5225	124.7080	180.1056	70.8309	70.8309	287.0673	0.0004	0.0224	0.0976	1.0000	1.0000	1.0000

Note: $N_k = 50$, $k = 3$, $f_s = 6000\,\mathrm{Hz}$, $\mathrm{SNR} = 0$.

characteristics. With the properly chosen algorithm parameters, MAFVRO algorithm can reasonably predict the normal modes of the system. The algorithm requires output data only and less computing effort than conventional EMA.

6. Conclusions

This work develops the modal parameter extraction method by using free vibration response data only. The system displacement response is assumed to be measured and input to the MAFVRO program, so as to predict the normal modes of the system. Some conclusions and recommendations are summarized as follows:

1. The proper selection of the sampling frequency and higher-order finite different formula in formulating the system response matrices is important. According to this study, the second-order central formula can be stuffiest for practical application, and the corresponding sampling frequency should be at least 8 times of the desired maximum frequency to ensure accurate prediction.
2. Either the started number of data point or the range of data points can be very flexibly selected and predict the modal parameters very well. In practice, only a few data points, for example 50 data points for each dof, are required.
3. The algorithm is tested and the feasibility is shown for a 3-dof and a 10-dof systems, and can be potentially extended to continuous systems. For a continuous system, the structure will be divided into grid to perform practical measurement at those M grid points. The response at each grid point can be measured and corresponding to a dof's response; therefore, the M dofs system can be equivalently considered. The proposed method can be applied to arbitrary structures theoretically.
4. Only proportional viscous damping is shown in this paper; however, the MAFVRO algorithm can be feasible for general (non-proportional) viscous damping case that is under investigation.
5. In practice, accelerometers are generally used to measure structural response. The formulation can be slightly revised to perform numerical integration of acceleration so as to obtain the velocity and displacement response matrices for modal parameter identification by MAFVRO algorithm.

References

[1] A.T.M.J.M. Huizinga, M.A.A. Van Ostaijen, G.L. Van Oosten Slingeland, A practical approach to virtual testing in automotive engineering, *Journal of Engineering Design* 13 (2002) 33–47.
[2] B.H. Kim, N. Stubbs, T. Park, A new method to extract modal parameters using output-only response, *Journal of Sound and Vibration* 282 (2005) 215–230.
[3] S.R. Ibrahim, E.C. Mikulcik, A method for the direct identification of vibration parameters from the free response, *Shock and Vibration Bulletin* 47 (2005) 183–198.
[4] R. Brinker, L. Zhang, P. Andersen, Modal identification from ambient responses using frequency domain decomposition, *Proceedings of 18th International Modal Analysis Conference*, San Antonio, TX, 2000, pp. 625–630.
[5] F. Shen, M. Zheng, D.F. Shi, F. Xu, Using the cross-correlation technique to extract modal parameters on response-only data, *Journal of Sound and Vibration* 259 (2003) 1165–1179.
[6] P. Mohanty, D.J. Rixen, Modified SSTD method to account for harmonic excitations during operational modal analysis, *Mechanism and Machine Theory* 39 (2004) 1247–1255.
[7] S.A. Zaghlool, Single-station time domain(SSTD) vibration testing technique: theory and application, *Journal of Sound and Vibration* 72 (1980) 205–234.
[8] P. Mohanty, D.J. Rixen, Operational modal analysis in the presence of harmonic excitation, *Journal of Sound and Vibration* 270 (2004) 93–109.
[9] D.J. Yu, W.X. Ren, EMD-based stochastic subspace identification of structures from operational vibration measurement, *Engineering Structures* 27 (2005) 1741–1751.
[10] W. Zhou, D. Chelidze, A new method for vibration modal analysis, *Proceeding of the SEM Annual Conference and Exposition on Experimental and Applied Mechanics*, Portland, OR, USA, 2005, pp. 390–391.
[11] B.F. Feeny, R. Kappagantu, On the physical interpretation of proper orthogonal modes in vibration, *Journal of Sound and Vibration* 211 (1998) 607–616.
[12] S. Han, B. Feeny, Application of proper orthogonal decomposition to structural vibration analysis, *Mechanical System and Signal Processing* 17 (2003) 989–1001.

[13] B.F. Feeny, Y. Liang, Interpreting proper orthogonal modes of randomly excited vibration system, *Journal of Sound and Vibration* 265 (2003) 953–966.

[14] G. Kerschen, J.G. Golinval, Comments on interpreting proper orthogonal modes of randomly excited linear vibration system, *Journal of Sound and Vibration* 274 (2004) 1091–1092.

[15] M.F.A. Azeez, A.F. Vakakis, Proper orthogonal decomposition(POD) of a class of vibroimpact oscillation, *Journal of Sound and Vibration* 240 (2001) 859–889.

[16] G. Kerschen, J.G. Golinval, Physical interpretation of the proper orthogonal modes using the singular value decomposition, *Journal of Sound and Vibration* 249 (2002) 849–865.

[17] A. Chakraborty, B. Basu, M. Mitra, Identification of modal parameters of a MDOF system by modified L–P wavelet packets, *Journal of Sound and Vibration* 295 (2006) 827–837.

[18] L. Meirovitch, *Principles and Techniques of Vibration*, Prentice-Hall, Inc., Englewood Cliffs, NJ, 1997.